G.O.Joe: A new non-commercial software tool for the processing of LA–ICP–MS trace element data

Florian **Altenberger** (1)* iD, Joachim **Krause** (2), Thomas **Auer** (3), Alexander **Auer** (3) and Jasper **Berndt** (4)

(1) Montanuniversität Leoben, Department Applied Geosciences and Geophysics, Chair of Resource Mineralogy, Peter Tunner-Straße 5, Leoben 8700, Austria
(2) Helmholtz-Zentrum Dresden-Rossendorf, Helmholtz Institute Freiberg for Resource Technology, Chemnitzer Straße 40, Freiberg 09599, Germany
(3) Moonshot Pioneers GmbH, Dorfbeuern 35, Dorfbeuern/Salzburg 5152, Austria
(4) Institute for Mineralogy, University of Münster, Corrensstraße 24, Münster 48149, Germany
* Corresponding author. e-mail: info@gojoe.software

A common problem of trace element measurements by LA-ICP-MS is the existence of interferences that cannot be resolved instrumentally. The software G.O.Joe is developed to calculate trace element mass fractions in solid samples analysed by LA-ICP-MS, offering the opportunity to correct for isobaric interference (including mass bias) and abundance sensitivity. Designed as a platform-independent web application, G.O.Joe is written in the Dart programming language and runs on all web browsers supported by Flutter (i.e., Chrome, Safari, Edge, Firefox) without the need for installation. G.O.Joe is freely accessible from any computer with an internet connection to facilitate immediate data evaluation and the efficient processing of large datasets ($>$ 400 analyses). G.O.Joe features an intuitive user interface that simplifies the selection of peak and background signals, import of instrument settings and reference material compositions to convert the measured raw signals into element mass fractions. Key functions of G.O.Joe are presented by processing the analysis of tungstates and silicates (i.e., scheelite and garnet) including specific correction methods to demonstrate their large effect on interfered masses/isotopes achievable with only little effort. This study introduces G.O.Joe as a simple, time-efficient and flexible software to significantly improve data quality in various trace element studies utilising LA-ICP-MS.

Keywords: data reduction software, laser ablation-inductively coupled plasma-mass spectrometry, correction methods, isobaric interference, abundance sensitivity, trace elements.

The coupling of laser ablation systems to inductively coupled plasma-mass spectrometers (LA-ICP-MS) was introduced in the 1980s (Gray 1985). Since then, it has evolved into an essential tool for the *in situ* chemical analysis of both natural and synthetic solid samples (e.g., Arrowsmith 1987, Günther *et al.* 1997, Jeffries *et al.* 1998, Russo *et al.* 2002, Sylvester and Jackson 2016). LA-ICP-MS allows fast and spatially resolved acquisition of trace element compositions in solid samples. Its application spans diverse fields, from chemistry and material science (Becker 2002a, Zheng *et al.* 2020) to geosciences (Sylvester 2001, 2008) and includes biological and environmental analysis (Durrant and Ward 2005) as well as bioimaging and forensic investigations (Orellana *et al.* 2013, López-Fernández *et al.* 2016).

LA-ICP-MS is frequently utilised in Earth sciences, for example, to study the physicochemical conditions of rock and mineral forming processes based on the distribution of trace elements or to trace chemical variations during complex mineral precipitation events (e.g., Jackson *et al.* 1992, Sylvester and Ghaderi 1997, Cook *et al.* 2016, Kozlik *et al.* 2016). The measurement of mineral trace element compositions has proven successful in mineral exploration and presents a potential approach to evaluating a broad spectrum of commodities through indicator minerals, such as apatite, garnet, spinel, scheelite, wolframite, rutile, magnetite, cassiterite, sphalerite etc. (e.g., Karimzadeh Somarin 2004, Goldmann *et al.* 2013, Dare *et al.* 2014, Wilkinson *et al.* 2015, Mao *et al.* 2016,

McClenaghan et al. 2017, Altenberger et al. 2021, Sciuba and Beaudoin 2021, Bertrandsson Erlandsson et al. 2022, Miranda et al. 2022).

The low detection levels and rapid analytical capabilities of ICP-MS, paired with the high-resolution *in situ* analysis on the tens of micrometre scale via laser ablation, offer significant advantages for the determination of trace element compositions over X-ray microanalysis either on scanning electron microscopes (SEM) or electron probe microanalysers (EPMA) and other techniques such as laser-induced breakdown spectroscopy (LIBS), secondary ion mass spectrometry (SIMS) etc. (e.g., Jackson et al. 1992, Eggins 2003, Jenner and Arevalo 2016, Chew et al. 2021). However, reliable measurement results are often compromised by isobaric and polyatomic interferences, abundance sensitivity as well as multiplicative effects of the ablated volume of the sample, instrumental sensitivity drift, matrix effects and elemental/isotopic fractionation (Longerich et al. 1996b, Becker 2002b, Guillong et al. 2011). Drift and matrix effects are commonly resolved by normalisation to an internal standard (Longerich et al. 1996a) but still a primary goal performing trace element measurement by LA-ICP-MS is to avoid any interference and fractionation effects by proper tuning of the instrumentation. Unfortunately, this is not always possible and thus, careful data processing is indispensable to comprehensively address all these challenges (Miliszkiewicz et al. 2015, Lin et al. 2016).

Over the last decades, several well-established software products for trace element data reduction have been developed to enhance productivity by automatically calculating, interpolating and applying various correction/calibration factors required for a proper evaluation of trace element data. GLITTER was one of the first software tools for processing LA-ICP-MS data, emphasising ease of use and real-time data reduction (Van Achterbergh et al. 2001, Griffin et al. 2008). Iolite advanced the field with more comprehensive features, including integration with the Igor Pro environment, offering improved data visualisation and flexibility, but in its latest version has transitioned to a faster platform based on C++ and Python (Paton et al. 2011). LADR was designed to enhance accessibility and precision for geochemical data, focusing on user-friendly interfaces and customisation for diverse analytical needs (Norris and Danyushevsky 2018). In addition, there are many other Python- or MATLAB-based software packages that provide features to increase the precision and accuracy of data evaluation (e.g., Guillong et al. 2008, Branson et al. 2019, Faltusová et al. 2022).

Recent studies on tungsten minerals with complex sample matrices have reported interference issues due to the high abundance of certain elements (e.g., Goldmann et al. 2013, Altenberger et al. 2024, Haupt et al. 2024). These issues arise from isobaric interferences and abundance sensitivity affecting nearby masses (see Appendix S1 in the electronic supplementary material for more information), particularly for critical elements such as In, Ga, Ta, Re, etc. Some of the software developers listed above already offer advanced products with comprehensive options for interference correction (e.g., Iolite or LADR). Premium software, however, is often limited to individual licenses and is not flexibly accessible to everyone from everywhere. Consequently, data reduction and interference correction often require manual processing using in-house spreadsheets, which is a time-intensive approach.

Here, we introduce G.O.Joe, a new software designed for the basic calculation of trace element contents from time-resolved signals measured by LA-ICP-MS. G.O.Joe allows essential corrections for interferences, including isobaric and abundance sensitivity, and is potentially applicable to all types of solid materials. The software enables fast and comprehensive data evaluation in just three steps, facilitating quantifiable and reproducible integration of LA-ICP-MS data. G.O.Joe intends to be a non-commercial software and was developed as a platform-independent web application written in the Dart programming language using Flutter, an open source framework by Google for building applications by a single codebase (Napoli 2019). Hence, G.O.Joe has the advantage of not requiring software installation to start with data evaluation, thereby providing a flexible tool of choice for both experienced operators of LA-ICP-MS as well as early-stage users. Data safety is preserved because neither the raw data nor the results are transferred to the G.O.Joe server. In this study, we will demonstrate the power of G.O.Joe by presenting its applications to two different types of potential indicator minerals, namely scheelite and garnet.

Materials and methods

The high-quality data processing and interference correction capabilities of G.O.Joe are illustrated with the following examples: (1) a scheelite analysis demonstrating how elements such as Ta (and Re) are influenced by abundance sensitivity due to its high W content and (2) a garnet analysis to demonstrate the effect of isobaric interference of ^{115}Sn on ^{115}In.

Example 1: Abundance sensitivity effect in scheelite analyses

Example 1 focuses on scheelite ($CaWO_4$), a tungstate mineral with a matrix composition known to present analytical challenges due to its high tungsten mass fraction (about 64% m/m). The dataset used in this study, includes 167 spot analyses of six natural scheelite samples from the Felbertal tungsten deposit in Austria and is part of the dataset from Haupt et al. (2024). The reference materials (RMs) used for quality control consist of two synthesised glasses (USGS GSD-1G and GSE-1G; Jochum et al. 2005a) and three matrix-matched in-house RMs (i.e., Ta-bearing Scheelite A and Scheelite B; Ta-free Scheelite S, Figure S1 in Appendix S1) made from natural scheelite crystals collected in the Felbertal deposit. Line scans on various pieces of the three in-house scheelite RMs indicate homogeneous trace element distribution. The preliminary results yielded a relative standard deviation from the mean of less than 15% for Scheelite A and less than 10% for Scheelite B and Scheelite S for element mass fractions well above the lower limit of quantification.

The example's focal point is the precise determination of Ta mass fractions. Along with Nb, the Nb-Ta fractionation in hydrothermal environments is frequently used to deduce ore-forming or petrogenetic processes (e.g., Dostal et al. 2009, Timofeev et al. 2017, Ballouard et al. 2020, Yin et al. 2022). However, the high tungsten content in scheelite causes a special type of interference known as abundance sensitivity (see Appendix S1 for more details about the calculation). This means there is an overlap on ^{181}Ta from the neighbouring ^{182}W and ^{183}W due to their high abundances. To ensure accurate Ta measurements, it is crucial to correct for abundance sensitivity effects. This not only increases the data quality but also the consistency over multiple datasets and is calculated by

$$I_x^{**} = I_{meas} - \left(I_y * A_x \right) \qquad (1)$$

where I_x^{**} is the abundance sensitivity corrected net count rate (e.g., ^{181}Ta, ^{185}Re etc.), I_{meas} is the measured net count rate of a given isotope of interest which is affected by abundance sensitivity, I_y is the measured net count rate of an adjacent isotope of the element which causes the abundance sensitivity (e.g., ^{183}W) and A_x is the abundance sensitivity factor.

Example 2: Isobaric interference of ^{115}Sn on ^{115}In in garnet

Example 2 addresses the microanalysis of silicate minerals demonstrated by analysing garnet collected from the Hämmerlein skarn deposit in the western Erzgebirge (Germany; Bauer et al. 2019, Korges et al. 2020; mineral composition between grossular and andradite; $Ca_3Al_2[SiO_4]_3$ - $Ca_3Fe^{3+}_2[SiO_4]_3$). Those garnets have high amounts of Sn causing a significant isobaric interference of ^{115}Sn on ^{115}In. This results in excessive indium contents if no correction is applied. Based on 143 garnet analyses, the application of the isobaric interference correction is presented together with the results for NIST SRM 612 glass, which is used as quality control material.

Indium as well as Ga, Ge, Co, PGE and REE are crucial for renewable energy technologies or high-tech applications (Werner et al. 2017, European Commission 2023). Therefore, it is imperative to deduce accurate results by correcting any interfered signal of these elements during data processing to ensure high quality results and to prevent any economic or scientific misinterpretation. The formula used to correct for isobaric interference is as follows

$$Ix_a^* = Ix_{meas} - \left(Iy_b * a_b \right) \qquad (2)$$

where Ix_a^* is the isobaric interference corrected net count rate of the interfered isotope x of element a, Ix_{meas} is the measured net count rate on mass x, Iy_b is the measured net count rate of the interfering element b on mass y (non-interfering isotope) and a_b is the correction factor determined by the ratio of the relative abundance of the isotopes x and y of element b.

Analytical set-up

Trace element compositions in scheelite and garnet were measured by LA-ICP-MS on polished sections at the LA-ICP-MS laboratory of the Institute for Mineralogy at the University of Münster, Germany. The analyses were carried out on a Thermo Fischer Element XR HR-ICP-MS coupled to a Teledyne Photon Machines Analyte G2 193 nm ArF-based excimer laser ablation system equipped with a HelEx2 ablation cell. Forward power was set to 1250 W and the scan was conducted in low-resolution (LR) e-scan mode. The Ar gas flow rates used were 16 l min^{-1} for the cooling gas, 1 l min^{-1} for the auxiliary and the sample gas and 0.65 l min^{-1} for the He gas. Each analysis was performed using a uniform spot size of 40 μm in diameter at 10 Hz with energy density of about 4 J cm^{-2} for 40 s after measuring the gas blank for 20 s followed by 15 s sample washout. Argon and helium gas flows, torch position and focusing potentials were adjusted by ablating the NIST SRM 612 to first optimise the intensities on ^{139}La and ^{232}Th and subsequently to minimise the oxide formation rate (^{232}Th/^{232}Th^{16}O < 0.05%).

Every twenty-five to forty unknown spots were bracketed with a set of RMs intended for calibration and quality control. For scheelite, the reference glass NIST SRM 612 was used as calibrant to correct the time-dependent sensitivity drift of the instrument and for garnet, the NIST SRM 610 glass was used. The pre-set element mass fraction values for the NIST SRMs in G.O.Joe are taken from Jochum *et al.* (2011) and for other commonly used RMs (e.g., USGS GSD-1G, GSE-1G etc.), the preferred values from the GeoReM database are used (see Jochum *et al.* 2005b). All intensities on the monitored masses measured on RMs and unknowns in examples 1 and 2 were normalised to ^{43}Ca and ^{29}Si, respectively, as internal standard. Major elements in scheelite and garnet were determined by EPMA WDS techniques prior to LA-ICP-MS analyses from the same spots ablated afterwards by the laser. Analytical conditions and EPMA instrument set-up follow the procedure described in Haupt *et al.* (2024).

Offline data processing and evaluation of trace element data was performed with the G.O.Joe software to test abundance sensitivity correction of W on Ta and Re in scheelite and isobaric interference correction of Sn on In in garnet. The results were filtered with an outlier criterion of 30%; i.e., signals that deviated more than 30% from the median of the count rates normalised to the internal standard were removed. An additional threshold filter was applied that requires a certain fraction of values passing the outlier test. This value was set to 25%. The lower limit of detection at 95% confidence was calculated on the basis of Poisson distribution statistics using the calculations from Pettke *et al.* (2012) for scheelite and Van Achterbergh *et al.* (2001) for garnet.

G.O.Joe's workflow

The workflow for data evaluation comprises three steps (Figure 1). First, a raw data visualisation provides time-resolved processing for every spot analysis and enables manual removal of individual signal intervals affected by inclusions or contaminations (Figure 2). Second, the software asks for information about the internal standard and RM used for calibration, outlier and threshold criteria and offers several options to calculate the limit of detection/quantification as well as the optional application of further interference correction algorithms. Third, the final step of automated calculation comprises the transformation of the raw signals into element contents and the determination of relative standard uncertainties based on counting statistics. The calculations follow the procedure described in Jochum *et al.* (2006) and Jochum *et al.* (2007) and consist of the
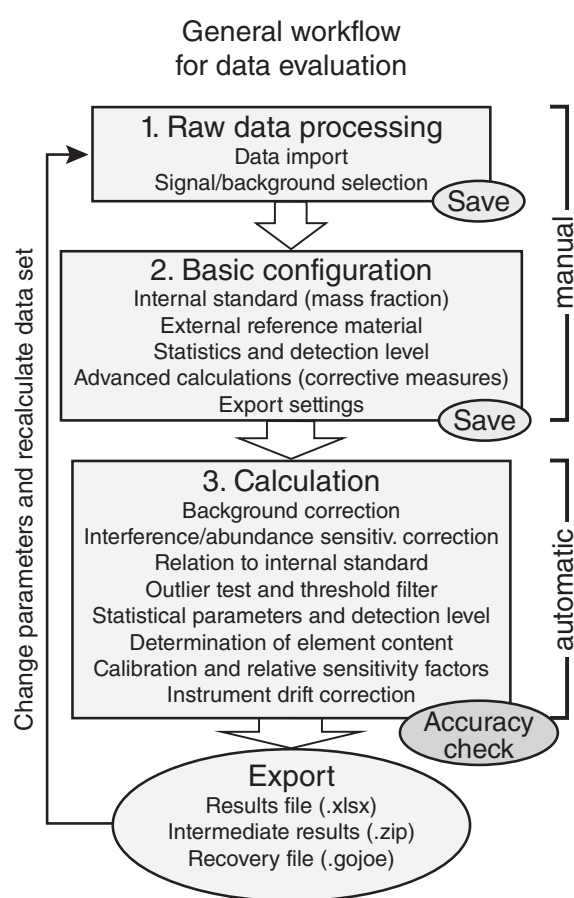

General workflow for data evaluation

Figure 1. Schematic overview of the general workflow for data evaluation with the G.O.Joe software, including the main steps of (manual) raw data processing and basic configuration followed by (automatic) data calculation. Before the export of the results, the accuracy check can be used to assess the data quality.

following consecutive steps applied to the entire dataset: (1) background correction, (2) optional correction of interferences (isobaric and abundance sensitivity), (3) count rate normalisation of monitored masses to that of the internal standard, (4) outlier filter, (5) threshold filter and (6) calculation of the limit of detection/quantification. A detailed description of the calculations performed by G.O.Joe is given in the online supporting information Appendix S1. More details about the exact workflow and data reduction with G.O.Joe can be viewed in Appendix S2.

Data reduction and evaluation procedure

G.O.Joe is a completely platform-independent web application that can be rendered on any web browser
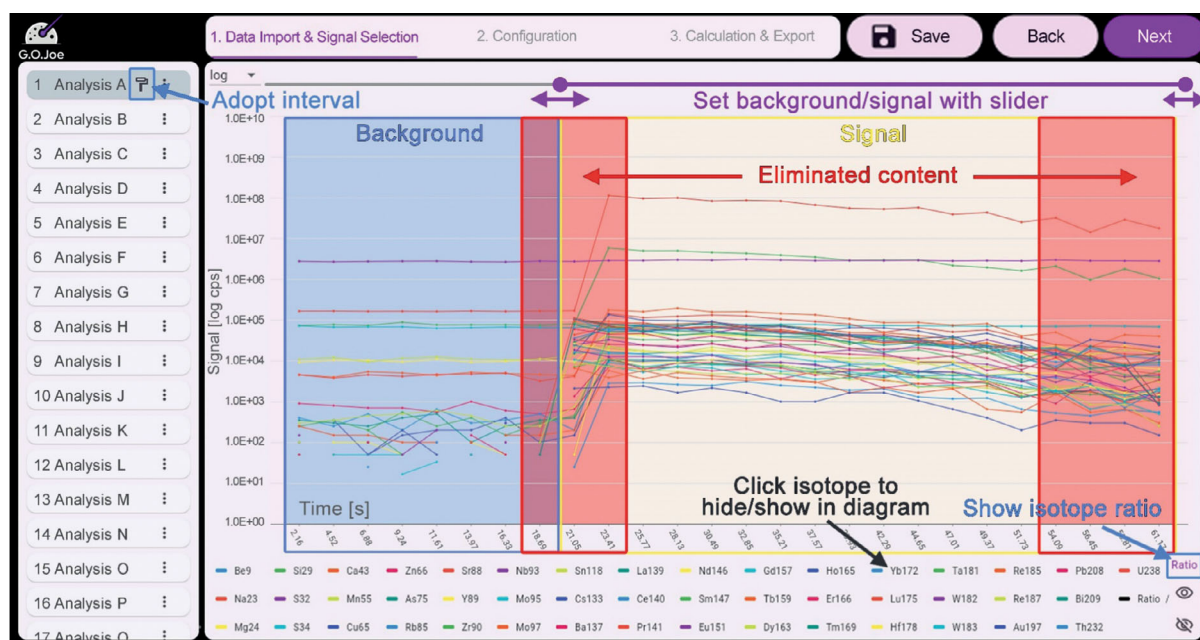
Figure 2. Graphical user interface of workflow step 1: Overview of the processing options in the signal selection-window. The diagram shows the time-resolved intensities of all measured masses ("isotopes") on a logarithmic (or linear) scale. All analyses are listed to the left of the diagram. The user can click through each analysis individually and specify the desired background (blue area) and signal (yellow area) intervals by using the slider. Individual sections may be excluded from further calculation (red area) by clicking on the desired intervals. Single mass signals can be hidden by clicking on the respective mass in the legend.

supported by Flutter (i.e., Chrome, Safari, Edge, Firefox). Nevertheless, it is recommended to use Chromium-based browsers (e.g., Chrome, Edge, Opera) in order to avoid complications that may occur more frequently with other browsers (e.g., copy-paste function not working). The G.O.Joe software supports the import of various raw data formats from different ICP-MS instruments (Agilent, Thermo Scientific etc.). No raw data files on the computer are modified by the application of G.O.Joe. During data reduction, a G.O.Joe-Recovery File can be downloaded at any time by clicking on "Save" (Figures 1 and 2). This file contains the current processing status of all measurement data and basic configurations. It can be uploaded again to continue with or re-evaluate any dataset.

Prerequisite for successful data evaluation is the preparation of the following information:

(1) a separate data file (.csv, .asc,. FIN2 etc.) for each spot analysis containing time versus intensity information;
(2) the analytical set-up and mass spectrometer settings (i.e., the measurement sequence of the unknowns/RMs, calibration reference material and peak dwell times);

(3) the mass fraction data (element/oxide content) of the internal standard from an external source (e.g., EPMA or stoichiometric values in μg g^{-1} or % *m/m*) in the measured sequence;
(4) if abundance sensitivity corrections are to be performed, a suitable RM must be analysed repeatedly during analysis that contains the element causing the mass abundance sensitivity as major component but is free of the trace elements, which need to be corrected in the unknown samples.

Please note that the naming of the uploaded data files is also important. To avoid problems, all file names must at least begin with the designation of the sample or RM and should be followed by a consecutive/custom numbering that is separated by an underscore (i.e., S1_1, S1_2, S2_1, S2_2, NIST612_1, NIST612_2, GSE-1G_1 etc.).

Signal selection and basic configuration

The evaluation procedure starts with the selection of peak and background parts of the individual analyses in a time-resolved mass plot (Figure 2). In a next step, the
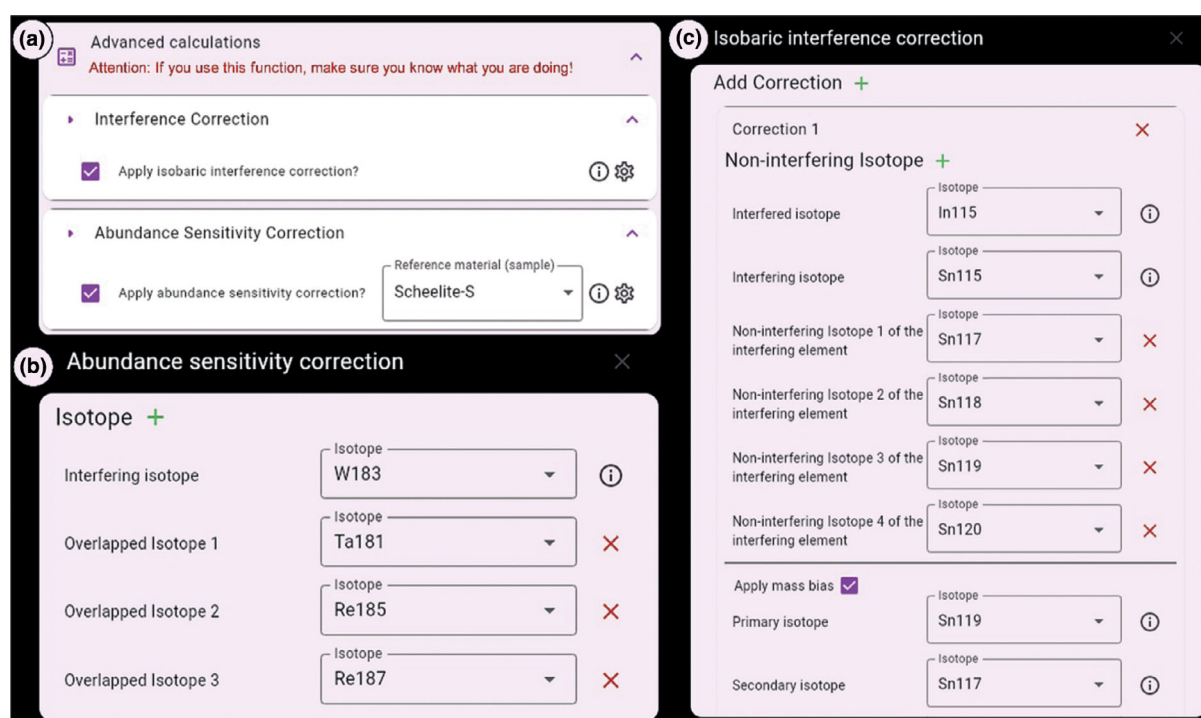
Figure 3. Graphical user interface of the advanced calculations-subwindow. (a) Overview of the advanced calculations tab. (b) Settings of the abundance sensitivity correction as used for scheelite in example 1. (c) Settings of the isobaric interference correction as used for garnet in example 2.

reference material for calibration and the internal standard element values need to be defined. Note that the preferred values of the most frequently used RMs were already imported from the GeoReM online database. Alternatively, the composition of a custom RM can be entered manually. Several filters for outlier, threshold and detection levels can be applied to the data. After the trace element values have been calculated, a quick quality check can be done by automatically comparing compositions of RM used as quality control material with GeoReM literature values. Finally, the results can be downloaded as an Excel file. The detailed description of the individual evaluation steps can be found in Appendix S2 and a step-by-step manual in Appendix S3.

Advanced calculations

For the more experienced users of G.O.Joe, advanced calculations can be conducted to correct for abundance sensitivity and isobaric interferences. In order to perform such corrections successfully, it is recommended to analyse suitable (matrix-matched or pure) RMs for calibration. The theory behind these calculations is mainly based on the equations given above (Equations 1 and 2) and is explained in Appendix S1. A detailed application description of the advanced calculation can be found in Appendix S2 and S3.

To apply the abundance sensitivity correction, activate the box on the left side of the tab and select the matrix-matched RM that is free of the element affected by the abundance sensitivity from the sample list (Figure 3a). In example 1, we correct the overlapped ^{181}Ta, ^{185}Re and ^{187}Re in scheelite and therefore use the Ta- and Re-free in-house RM Scheelite S. Open the settings to define the interfering isotope (i.e., ^{183}W) and the overlapped isotope(s) (e.g., ^{181}Ta, ^{185}Re etc.; Figure 3b).

The isobaric interference correction is applied by creating a new correction using "Add correction" and selecting the appropriate isotopes (Figure 3c). In example 2, we correct garnet analyses because In is overlapped by Sn. Therefore, select the interfered In isotope (i.e., ^{115}In) as well as the interfering Sn isotope (i.e., ^{115}Sn) in addition to the non-interfering isotopes of Sn (e.g., ^{117}Sn, ^{118}Sn etc.). Note that this is only possible if the interfering element has been measured on several masses. Moreover, it is recommended to consider the mass-based fractionation for the isotopes of the interfering element during the isobaric interference correction. This function must be activated

separately by checking the "Apply mass bias" box under the last non-interfering isotope. For the calculation, the definition of a primary (e.g., ^{119}Sn) and a secondary (i.e., ^{117}Sn) non-interfering isotope of the interfering element is necessary (Figure 3c).

Results and discussion

Analysis of scheelite applying abundance sensitivity correction

Tantalum in scheelite measurements from example 1 shows that the mass fractions without abundance sensitivity correction are above the detection limit in all analyses and range between 0.64 and 280 µg g^{-1}. When applying the abundance sensitivity correction (Appendix S2), however, most of the corrected Ta values between 1.1 and 0.78 µg g^{-1} will be eliminated completely because they fall below the limit of detection calculated for each analysis based on the interference corrected signal. This shows that the abundance sensitivity of W on Ta can cause false values of up to one order at a corrected mass fraction of 1 µg g^{-1} and must be considered especially in W-rich samples with low Ta mass fractions.

The effect of abundance sensitivity becomes even clearer when the corrected values for Ta are compared with the uncorrected results for Ta (Figure 4a). Our dataset shows that the relative correction factor increases steadily with a decreasing mass fraction of Ta. The correction is most clearly visible from an uncorrected Ta content of < 2.5 µg g^{-1} (i.e., about the uncorrected Ta value of Scheelite A). For samples with uncorrected results for Ta between 2.5 and 1.1 µg g^{-1}, the values are corrected by 35 to 80% with decreasing Ta content; uncorrected values below 1.1 µg g^{-1} usually fall below the detection limit or are already filtered out in the outlier/threshold test. For higher uncorrected Ta levels (>2.5 µg g^{-1}), the values are corrected by 30 to 10%.

The reproducible values of two Ta-bearing in-house RMs (Scheelite A and Scheelite B; Figure 4a) from the Felbertal deposit serve as monitoring of the abundance sensitivity correction, whereas the correction factor A_x is determined by regular measurements of the Ta-free Scheelite S. For Scheelite A, the uncorrected Ta mass fraction of 2.7 ± 0.08 µg g^{-1} is corrected to 1.9 ± 0.09 µg g^{-1}. Scheelite B has lower uncorrected values of 1.2 ± 0.04 µg g^{-1} that are corrected to 0.3 ± 0.05 µg g^{-1}. In contrast, the synthetic glass RMs GSD-1G and GSE-1G are not affected by the correction, which is expected given the low mass fraction of

W (43 and 430 µg g^{-1}) relative to Ta (40 and 390 µg g^{-1}). Both RMs plot on the 1:1 line in the diagram at Ta values of 40 ± 0.87 µg g^{-1} and 410 ± 5.5 µg g^{-1}, respectively (i.e., 5 to 10% deviation from the literature values).

The correctness of the data evaluation with G.O.Joe is confirmed by comparing the calculated LA-ICP-MS results of Mo with those from the same scheelite spots by previous electron probe microanalysis. Most samples show an agreement of around 10% between the Mo mass fraction determined with both instruments (Figure 4b). The quality check of GSD-1G illustrates that the deviation between the calculated results and the preferred values from GeoReM is better than 10% (Figure 4c).

Analysis of garnet applying isobaric interference correction

In some garnet analyses from example 2, the uncorrected results for In range from 10 to 65 µg g^{-1}. After applying interference corrections, these values decrease to less than 5 to 10 µg g^{-1}, as illustrated in Figure 5a. The NIST SRM 612 plotting at the 1:1 line remains unaffected by the correction and the In analyses deviate between 0.1 and 6% from the literature value. The comparison of the results calculated with G.O.Joe and the results of the previously used in-house spreadsheet (MS Excel) shows an agreement of more than 99% (Figure 5b), supporting also the validity of the calculations performed by G.O.Joe. A full comparison of all intermediate results is provided in Appendix S4 for the analysis of garnet sample GRT-27 (see arrow in Figure 5a).

Different methods were used to calculate the isobaric interference correction and can be looked up in Appendix S2. The correction was carried out both with the basic approach that uses only the natural isotope ratio of the interfering ^{115}Sn (i.e., on ^{115}In) and the non-interfering Sn isotopes (e.g., ^{117}Sn, ^{118}Sn etc.) as well as the mass bias approach that considers the mass-based fractionation of the Sn isotopes (Figure 6).

The comparison of the natural isotope ratio of ^{113}In/^{115}In (0.045) and the ratio of the uncorrected count rates measured on masses 113 and 115 shows that both the investigated garnet samples and the RMs NIST SRM 610 and NIST SRM 612 deviate significantly from the natural ratio. The check of the mass ratio 117/120 corresponds to the natural isotopic ratio of ^{117}Sn/^{120}Sn (0.236) so that either ^{117}Sn or ^{120}Sn are suitable as a correction basis for ^{115}Sn on ^{115}In. By applying the isobaric interference correction (^{117}Sn used as non-interfering
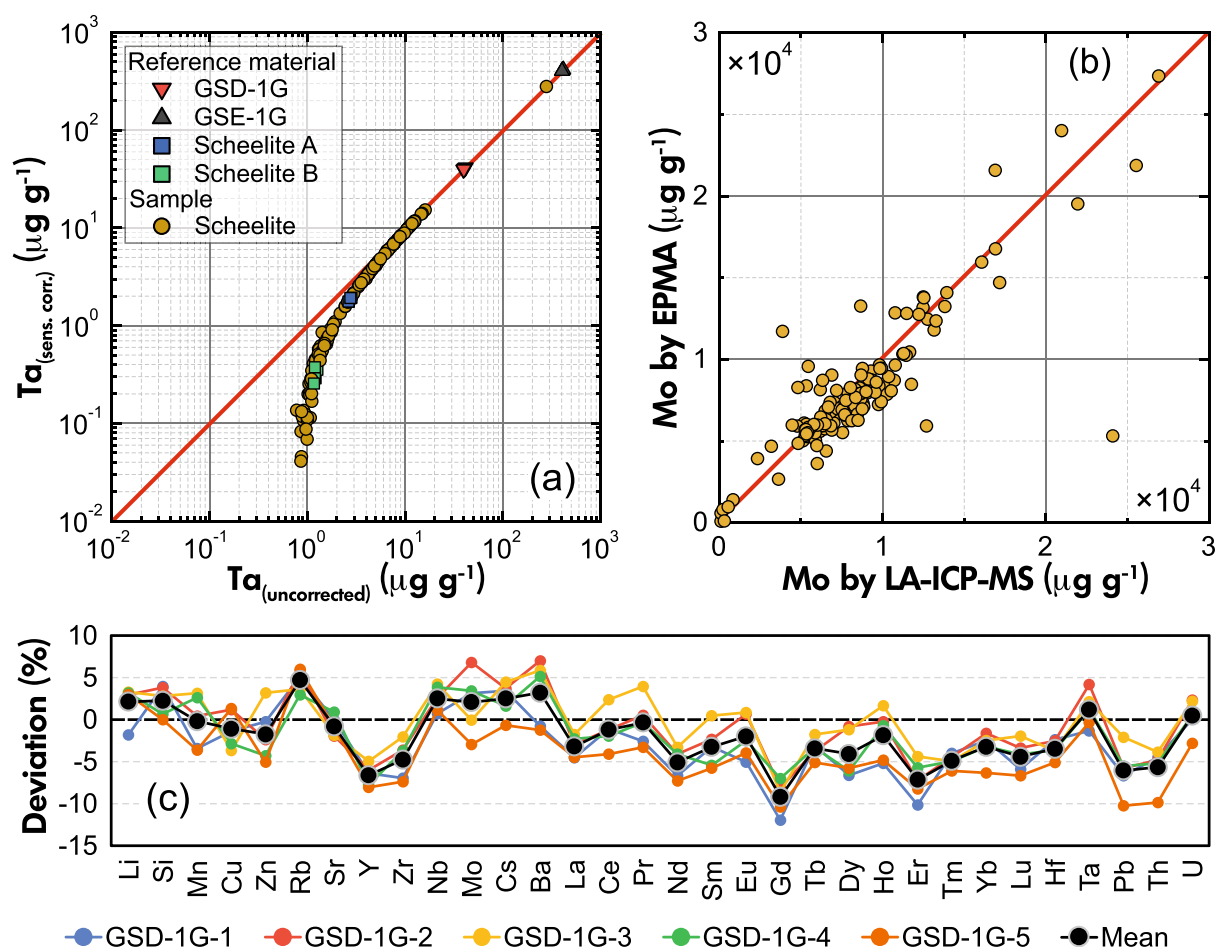
Figure 4. Results of example 1: Binary plots of (a) uncorrected Ta values versus Ta corrected for abundance sensitivity in scheelite and (b) Mo determined by LA-ICP-MS and EPMA. (c) Quality check of the measured values for the reference material GSD-1G showing the deviation (in %) based on literature values (Jochum *et al.* 2005b). Deviation = (value$_{measured}$ - value$_{literature}$) / value$_{literature}$ * 100.

isotope), the ratio can be corrected to the natural isotopic ratio in most analyses (Figure 6).

Based on the different non-interfering isotopes used for the correction, small differences may arise, especially for the more strongly corrected In values. In our example, the difference between the corrected results for the same measurement is usually < 0.5% and is therefore within the standard uncertainty of the individual analysis (Figure 5a). Only a minority of the corrected results show differences of up to 7%. Hence, it is advisable to include, if available, several non-interfering isotopes of the interfering element to compare the corrected results with each other in order to verify that the included isotopes are not affected by interference and to select the optimal isotopes for correction.

The comparison between the simple corrections (i.e., using only isotope ratios) and the correction considering

mass-based fractionation shows only small differences of about 0.4%, which are also within the standard uncertainty of single measurements (Figure 5a). The maximum difference in our dataset is around 11% and relates to individual, unstable measurement signals of the masses used for the correction. For the rather high mass of In and Sn (between 115 and 120) there are only slight differences between the basic and the mass bias correction method. This can be attributed to the fact that the mass discrimination effect decreases with increasing mass of isotopes. For isotope ratios at lower masses (around < 20) a mass discrimination higher than 10% is usually observed in ICP-MS (Becker 2002b), however, mass bias in any mass range may also depend on specific ICP-MS instrumentation and tuning. Thus, it is generally recommended to apply a mass bias correction and carefully examine the differences between the two approaches particularly when correcting for lighter elements. Mind that an adequate amount of non-interfering isotopes
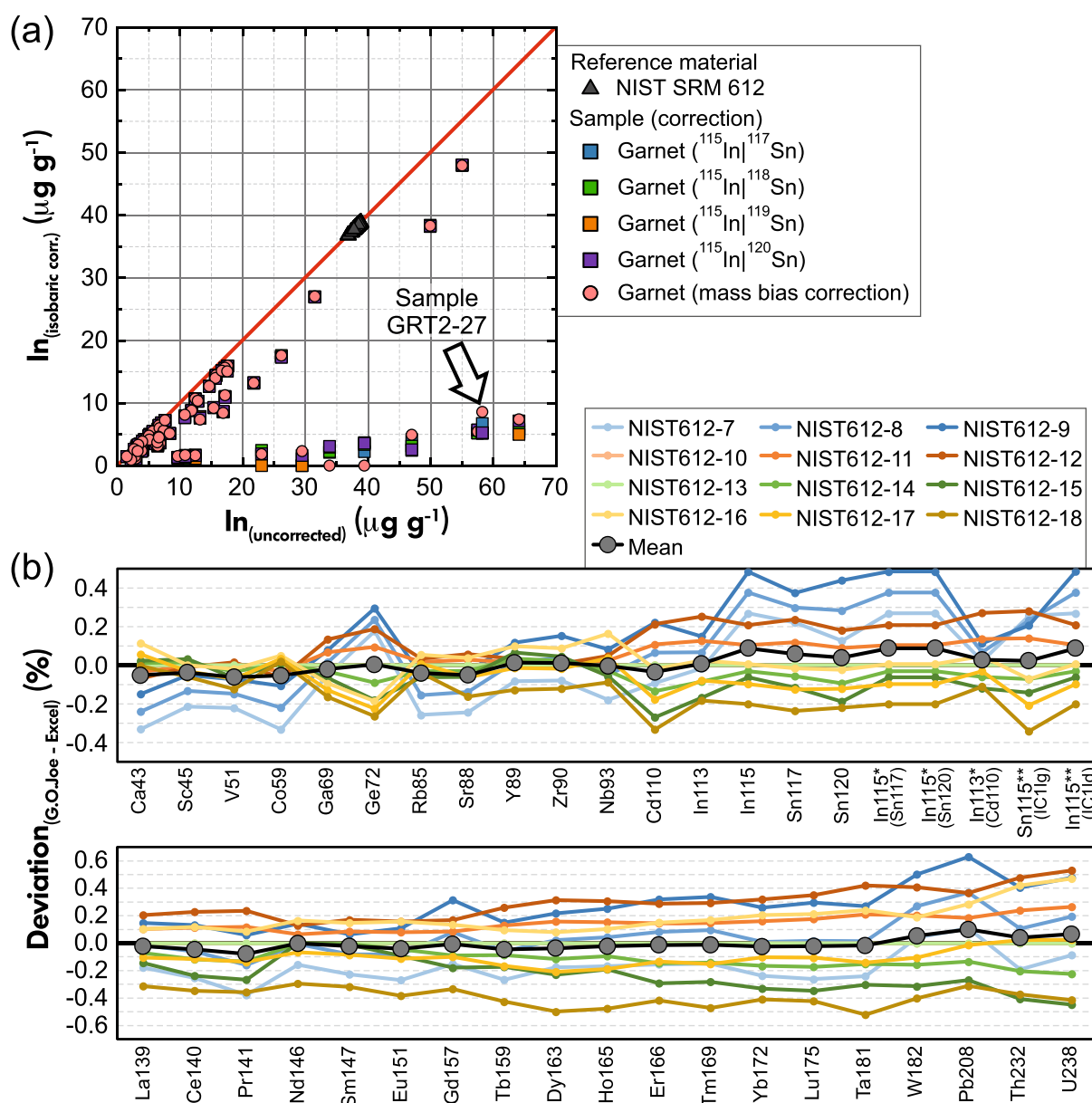
Figure 5. Results of example 2: Binary plot of uncorrected In values versus isobaric interference corrected In contents in garnet. Both correction approaches are shown in the diagram; simple correction by using the isotopic ratio of ^{115}Sn and several other Sn isotopes (e.g., ^{117}Sn, ^{118}Sn etc.; square symbols) and mass bias correction (red circles). (b) Comparison of the results calculated automatically with G.O.Joe and manually using an in-house MS Excel spreadsheet. Deviation = (results$_{G.O.Joe}$ - results$_{Excel}$) / results$_{Excel}$ * 100.

must be included in the analytical session to achieve the most accurate results.

Conclusions and future developments

G.O.Joe is an intuitive software for data reduction of LA-ICP-MS trace element analysis, incorporating various interference correction methods. It is a non-commercial application that offers free dataset evaluations and subsequent reprocessing with the downloadable G.O.Joe-Recovery File. Programmed in Flutter, G.O.Joe is accessible online without the need for installation, enabling usage from any location with internet connection. The only prerequisite is a data format compatible with the software. We ensure that no raw data or results are retained on G.O.Joe's servers
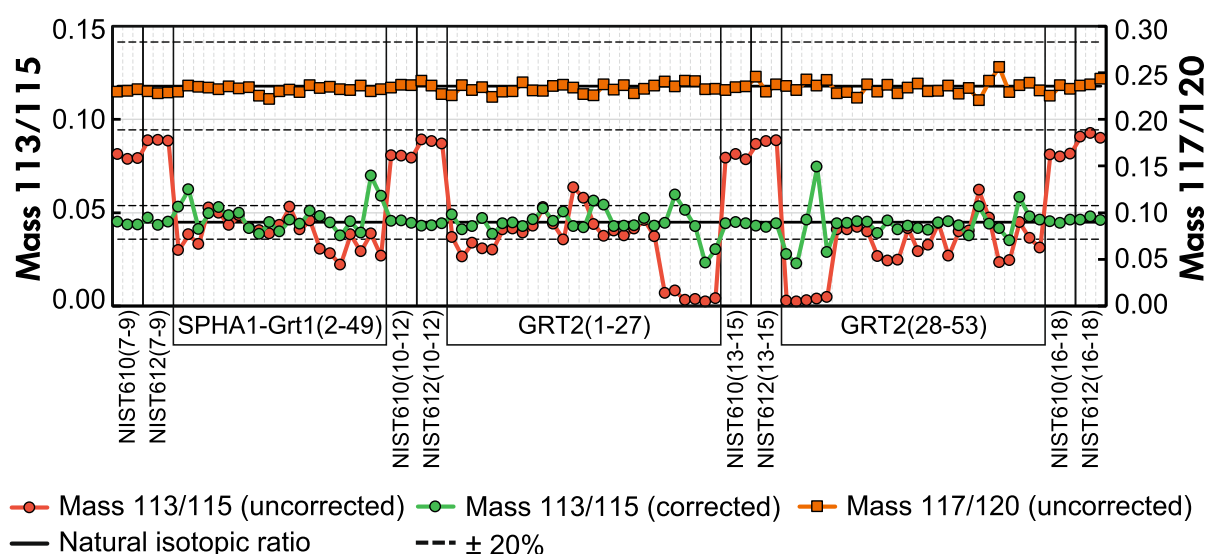
Figure 6. Mass ratios based on count rates per second illustrating the effect of isobaric interference correction for ^{113}In/^{115}In.

post-session or after an internet disconnection, thereby maximising data security. Updates and new software features will be regularly posted on the website.

The examples of scheelite and garnet demonstrate that G.O.Joe is both simple and user-friendly. It facilitates the correction of interfered elements with minimal effort, a task that previously necessitated manual raw data processing and the use of tools like in-house spreadsheets. Consequently, the software substantially enhances data quality and consistency over multiple datasets in various trace element studies utilising LA-ICP-MS. The correctness of the calculations performed by G.O.Joe can be confirmed by the exact agreement of the intermediate results with the manual evaluation and the strong correlation of minor element mass fractions determined by routine EPMA measurements prior to LA-ICP-MS.

G.O.Joe will remain a work in progress. The software is of course constantly evolving and some problems have not yet been fully resolved. New approaches to correct other interference problems may include a polyatomic (or molecular) interference correction, for which we are eager to develop a universal correction method. In addition, there is potential for development in dealing with the propagation of uncertainties in the next software versions. Many more features can be developed in the future to provide a comprehensive software tool for everyone, such as the upload of logbooks for renaming data files, plotting diagrams, the extension of file types from different ICP-MS

systems that are not yet supported by G.O.Joe etc. Thus, we invite everyone to get in touch with us to help develop the software by expanding its scope and implementing more features. The latest version of G.O.Joe is available at https://www.gojoe.software.

Acknowledgements

Data availability statement

Data available on request from the authors.

References

Altenberger F., Raith J.G., Weilbold J., Auer C., Knoll T., Paulick H., Schedl A., Aupers K., Schmidt S. and Neinavaie H. (2021)
Casting new light on tungsten deposits in the eastern Alps. Zeitschrift der Deutschen Gesellschaft für Geowissenschaften, 172, 63–72.

Altenberger F., Krause J., Wintzer N.E., Iglseder C., Berndt J., Bachmann K. and Raith J.G. (2024)
Polyphase stratabound scheelite-ferberite mineralization at Mallnock, eastern Alps, Austria. Mineralium Deposita, 59, 1109–1132.

Arrowsmith P. (1987)
Laser ablation of solids for elemental analysis by inductively coupled plasma-mass spectrometry. Analytical Chemistry, 59, 1437–1444.

Ballouard C., Massuyeau M., Elburg M.A., Tappe S., Viljoen F. and Brandenburg J.-T. (2020)
The magmatic and magmatic-hydrothermal evolution of felsic igneous rocks as seen through Nb-Ta geochemical fractionation, with implications for the origins of rare-metal mineralizations. Earth-Science Reviews, 203, 103115.

Bauer M.E., Seifert T., Burisch M., Krause J., Richter N. and Gutzmer J. (2019)
Indium-bearing sulfides from the Hämmerlein skarn deposit, Erzgebirge, Germany: Evidence for late-stage diffusion of indium into sphalerite. Mineralium Deposita, 54, 175–192.

Becker J.S. (2002a)
Applications of inductively coupled plasma-mass spectrometry and laser ablation inductively coupled plasma-mass spectrometry in materials science. Spectrochimica Acta Part B, 57, 1805–1820.

Becker J.S. (2002b)
State-of-the-art and progress in precise and accurate isotope ratio measurements by ICP-MS and LA-ICP-MS Plenary Lecture. Journal of Analytical Atomic Spectrometry, 17, 1172–1185.

Bertrandsson Erlandsson V., Wallner D., Ellmies R., Raith J.G. and Melcher F. (2022)
Trace element composition of base metal sulfides from the sediment-hosted Dolostone Ore Formation (DOF) Cu-Co deposit in northwestern Namibia: Implications for ore genesis. Journal of Geochemical Exploration, 243, 107105.

Branson O., Fehrenbacher J.S., Vetter L, Sadekov A.Y., Eggins S.M. and Spero H.J. (2019)
LAtools: A data analysis package for the reproducible reduction of LA-ICP-MS data. Chemical Geology, 504, 83–95.

Chew D., Drost K., Marsh J.H. and Petrus J.A. (2021)
LA-ICP-MS imaging in the geosciences and its applications to geochronology. Chemical Geology, 559, 119917.

Cook N., Ciobanu C.L., George L, Zhu Z.-Y., Wade B. and Ehrig K. (2016)
Trace element analysis of minerals in magmatic-hydrothermal ores by laser ablation-inductively coupled plasma-mass spectrometry: Approaches and opportunities. Minerals, 6, 111.

Dare S.A.S., Barnes S.-J., Beaudoin G., Méric J., Boutroy E. and Potvin-Doucet C. (2014)
Trace elements in magnetite as petrogenetic indicators. Mineralium Deposita, 49, 785–796.

Dostal J., Kontak D. and Chatterjee A.K. (2009)
Trace element geochemistry of scheelite and rutile from metaturbidite-hosted quartz vein gold deposits, Meguma Terrane, Nova Scotia, Canada: Genetic implications. Mineralogy and Petrology, 97, 95–109.

Durrant S.F. and Ward N.I. (2005)
Recent biological and environmental applications of laser ablation inductively coupled plasma-mass spectrometry (LA-ICP-MS). Journal of Analytical Atomic Spectrometry, 20, 821–829.

Eggins S.M. (2003)
Laser ablation ICP-MS analysis of geological materials prepared as lithium borate glasses. Geostandards Newsletter: The Journal of Geostandards and Geoanalysis, 27, 147–162.

European Commission (2023)
Study on the critical raw materials for the EU 2023 – Final Report. Directorate-General for Internal Market, Industry, Entrepreneurship and SMEs, Joint Research Centre Directorate GROW.I; Unit GROW.I.1 - Energy-intensive Industries, Raw Materials and Hydrogen (Brussels), 152pp.

references

Faltusová V., Vaculovič T., Holá M. and Kanický V. (2022)
Ilaps – Python software for data reduction and imaging with LA-ICP-MS. Journal of Analytical Atomic Spectrometry, 37, 733–740.

Goldmann S., Melcher F., Gäbler H.-E., Dewaele S., Clercq F.D. and Muchez P. (2013)
Mineralogy and trace element chemistry of ferberite/reinite from tungsten deposits in central Rwanda. Minerals, 3, 121–144.

Gray A.L. (1985)
Solid sample introduction by laser ablation for inductively coupled plasma source mass spectrometry. Analyst, 110, 551–556.

Griffin W.L., Powell W.J., Pearson N.J. and O'Reilly S.Y. (2008)
GLITTER: Data reduction software for laser ablation ICP-MS. In: Sylvester P. (ed.), Laser ablation ICP-MS in the Earth Sciences: Current practices and outstanding issues. Mineralogical Association of Canada, Short Course Series 40, 307–311.

Guillong M., Meier D., Allan M., Heinrich C. and Yardley B. (2008)
SILLS: A MATLAB-based program for the reduction of laser ablation ICP-MS data of homogeneous materials and inclusions. In: Sylvester P. (ed.), Laser ablation ICP-MS in the Earth Sciences: Current practices and outstanding issues. Mineralogical Association of Canada, Short Course Series 40, 328–333.

Guillong M., Danyushevsky L., Walle M. and Raveggi M. (2011)
The effect of quadrupole ICP-MS interface and ion lens design on argide formation. Implications for LA-ICP-MS analysis of PGE's in geological samples. Journal of Analytical Atomic Spectrometry, 26, 1401–1407.

Günther D., Frischknecht R., Heinrich C.A. and Kahlert H.-J. (1997)
Capabilities of an argon fluoride 193 nm excimer laser for laser ablation inductively coupled plasma-mass spectometry microanalysis of geological materials. Journal of Analytical Atomic Spectrometry, 12, 939–944.

Haupt C.P., Krause J., Schulz B., Götze J., Chischi J., Berndt J., Klemme S., Schmidt S., Aupers K. and Reinhardt N. (2024)
New insights on the formation of the polymetamorphic Felbertal tungsten deposit (Austria, Eastern Alps) revealed by CL, EPMA, and LA-ICP-MS investigation. Mineralium Deposita. https://doi.org/10.1007/s00126-024-01284-1

Jackson S.E., Longerich H.P., Dunning G.R. and Fryer B.J. (1992)
The application of laser-ablation microprobe - inductively coupled plasma-mass spectrometry (LAM-ICP-MS) to in situ trace-element determinations in minerals. The Canadian Mineralogist, 30, 1049–1064.

Jeffries T.E., Jackson S.E. and Longerich H.P. (1998)
Application of a frequency quintupled Nd:YAG source ($\lambda = 213$ nm) for laser ablation inductively coupled plasma-mass spectrometric analysis of minerals. Journal of Analytical Atomic Spectrometry, 13, 935–940.

Jenner F.E. and Arevalo R.D., Jr. (2016)
Major and trace element analysis of natural and experimental igneous systems using LA-ICP-MS. Elements, 12, 311–316.

Jochum K.P., Willbold M., Raczek I., Stoll B. and Herwig K. (2005a)
Chemical characterisation of the USGS reference glasses GSA-1G, GSC-1G, GSD-1G, GSE-1G, BCR-2G, BHVO-2G and BIR-1G using EPMA, ID-TIMS, ID-ICP-MS and LA-ICP-MS. Geostandards and Geoanalytical Research, 29, 285–302.

Jochum K.P., Nohl U., Herwig K., Lammel E., Stoll B. and Hofmann A.W. (2005b)
GeoReM: A new geochemical database for reference materials and isotopic standards. Geostandards and Geoanalytical Research, 29, 333–338.

Jochum K.P., Stoll B., Herwig K. and Willbold M. (2006)
Improvement of in situ Pb isotope analysis by LA-ICP-MS using a 193 nm Nd:YAG laser. Journal of Analytical Atomic Spectrometry, 21, 666–675.

Jochum K.P., Stoll B., Herwig K. and Willbold M. (2007)
Validation of LA-ICP-MS trace element analysis of geological glasses using a new solid-state 193 nm Nd: YAG laser and matrix-matched calibration. Journal of Analytical Atomic Spectrometry, 22, 112–121.

Jochum K.P., Weis U., Stoll B., Kuzmin D., Yang Q., Raczek I., Jacob D.E., Stracke A., Birbaum K., Frick D.A., Günther D. and Enzweiler J. (2011)
Determination of reference values for NIST SRM 610–617 glasses following ISO guidelines. Geostandards and Geoanalytical Research, 35, 397–429.

Karimzadeh Somarin A. (2004)
Garnet composition as an indicator of Cu mineralization: Evidence from skarn deposits of NW Iran. Journal of Geochemical Exploration, 81, 47–57.

Korges M., Weis P., Lüders V. and Laurent O. (2020)
Sequential evolution of Sn-Zn-In mineralization at the skarn-hosted Hämmerlein deposit, Erzgebirge, Germany, from fluid inclusions in ore and gangue minerals. Mineralium Deposita, 55, 937–952.

Kozlik M., Raith J.G. and Gerdes A. (2016)
U-Pb, Lu-Hf and trace element characteristics of zircon from the Felbertal scheelite deposit (Austria): New constraints on timing and source of W mineralization. Chemical Geology, 421, 112–126.

Lin J., Liu Y., Yang Y. and Hu Z. (2016)
Calibration and correction of LA-ICP-MS and LA-MC-ICP-MS analyses for element contents and isotopic ratios. Solid Earth Sciences, 1, 5–27.

Longerich H.P., Günther D. and Jackson S.E. (1996a)
Elemental fractionation in laser ablation inductively coupled plasma-mass spectrometry. Fresenius' Journal of Analytical Chemistry, 355, 538–542.

Longerich H.P., Jackson S.E. and Günther D. (1996b)
Inter-laboratory note. Laser ablation inductively coupled plasma-mass spectrometric transient signal data

references

acquisition and analyte concentration calculation. **Journal of Analytical Atomic Spectrometry**, 11, 899–904.

López-Fernández H., de S. Pessôa G., Arruda M.A.Z., Capelo-Martínez J.L, Fdez-Riverola F., Glez-Peña D. and Reboiro-Jato M. (2016)
LA-iMageS: A software for elemental distribution bioimaging using LA-ICP-MS data. **Journal of Cheminformatics**, 8, 65.

Mao M., Rukhlov A., Rowins S., Spence J. and Coogan L. (2016)
Apatite trace element compositions: A robust new tool for mineral exploration. **Economic Geology**, 111, 1187–1222.

McClenaghan M.B., Parkhill M., Pronk A., Seaman A., McCurdy M. and Leybourne M. (2017)
Indicator mineral and geochemical signatures associated with the Sisson W-Mo deposit, New Brunswick, Canada. Geochemistry: Exploration, **Environment, Analysis**, 17, 297–313.

Miliszkiewicz N., Walas S. and Tobiasz A. (2015)
Current approaches to calibration of LA-ICP-MS analysis. **Journal of Analytical Atomic Spectrometry**, 30, 327–338.

Miranda A.C.R., Beaudoin G. and Rottier B. (2022)
Scheelite chemistry from skarn systems: Implications for ore-forming processes and mineral exploration. **Mineralium Deposita**, 57, 1469–1497.

Napoli M.L. (2019)
Introducing flutter and getting started. In: Napoli M.L. (ed.), Beginning Flutter®: A Hands On Guide To App Development. Wiley (Indianapolis), 1–23.

Norris A.C. and Danyushevsky L. (2018)
Towards estimating the complete uncertainty budget of quantified results measured by LA-ICP-MS. **Goldschmidt** (Boston, 2018-08-12).

Orellana F.A., Gálvez C.G., Orellana F.A., Gálvez C.G., Roldán M.T., Garáía-Ruiz C., Roldán M.T. and Garáía-Ruiz C. (2013)
Applications of laser ablation-inductively coupled plasma-mass spectrometry in chemical analysis of forensic evidence. **TrAC Trends in Analytical Chemistry**, 42, 1–34.

Paton C., Hellstrom J., Paul B., Woodhead J. and Hergt J. (2011)
Iolite: Freeware for the visualisation and processing of mass spectrometric data. **Journal of Analytical Atomic Spectrometry**, 26, 2508–2518.

Pettke T., Oberli F., Audétat A., Guillong M., Simon A.C., Hanley J.J. and Klemm L.M. (2012)
Recent developments in element concentration and isotope ratio analysis of individual fluid inclusions by laser ablation single and multiple collector ICP-MS. **Ore Geology Reviews**, 44, 10–38.

Russo R.E., Mao X., Gonzalez J.J. and Mao S.S. (2002)
Femtosecond laser ablation ICP-MS. **Journal of Analytical Atomic Spectrometry**, 17, 1072–1075.

Sciuba M. and Beaudoin G. (2021)
Texture and trace element composition of rutile in orogenic gold deposits. **Economic Geology**, 116, 1865–1892.

Sylvester P.J. and Ghaderi M. (1997)
Trace element analysis of scheelite by excimer laser ablation-inductively coupled plasma-mass spectrometry (ELA-ICP-MS) using a synthetic silicate glass standard. **Chemical Geology**, 141, 49–65.

Sylvester P.J. (2001)
Laser ablation ICP-MS in the Earth sciences: Principles and applications. **Mineralogical Association Canada Short Course Series 29**, 243pp.

Sylvester P.J. (2008)
Laser ablation ICP-MS in the Earth sciences: Current practices and outstanding issues. **Mineralogical Association Canada Short Course Series 40**, 356pp.

Sylvester P.J. and Jackson S.E. (2016)
A brief history of laser ablation inductively coupled plasma-mass spectrometry (LA-ICP-MS). **Elements**, 12, 307–310.

Timofeev A., Migdisov A.A. and Williams-Jones A.E. (2017)
An experimental study of the solubility and speciation of tantalum in fluoride-bearing aqueous solutions at elevated temperature. **Geochimica et Cosmochimica Acta**, 197, 294–304.

Van Achterbergh E., Ryan C.G. and Griffin W.L. (2001)
GLITTER: On-line interactive data reduction for the laser ablation ICP-MS microprobe. **Macquarie Research Ltd.** (Sydney), 71pp.

Werner T.T., Mudd G.M. and Jowitt S.M. (2017)
The world's by-product and critical metal resources part III: A global assessment of indium. **Ore Geology Reviews**, 86, 939–956.

Wilkinson J.J., Chang Z., Cooke D.R., Baker M.J., Wilkinson C.C., Inglis S., Chen H. and Bruce Gemmell J. (2015)
The chlorite proximitor: A new tool for detecting porphyry ore deposits. **Journal of Geochemical Exploration**, 152, 10–26.

Yin R., Huang X., Wang R., Sun X.-M., Tang Y., Wang Y. and Xu Y.-G. (2022)
Rare-metal enrichment and Nb–Ta fractionation during magmatic–hydrothermal processes in rare-metal granites: Evidence from zoned micas from the Yashan pluton, south China. **Journal of Petrology**, 63, 1–28.

![GEOSTANDARDS and GEOANALYTICAL RESEARCH logo]

references

Zheng L.-N., Feng L.-X., Shi J.-W., Chen H.-Q., Wang B., Wang M., Wang H.-F. and Feng W.-Y. (2020)
Single-cell isotope dilution analysis with LA-ICP-MS: A new approach for quantification of nanoparticles in single cells. Analytical Chemistry, 92, 14339–14345.

Supporting information

The following supporting information may be found in the online version of this article:

Appendix S1. Calculations performed by the software.

Appendix S2. Data reduction and evaluation procedure.

Appendix S3. Step-by-step software operating manual.

Appendix S4. Intermediate results for sample GRT2-27.

This material is available from: http://onlinelibrary.wiley.com/doi/10.1111/ggr.12596/abstract (This link will take you to the article abstract).